To be presented at MILCOM 2009 in Boston.

HIGH PERFORMANCE MICROWAVE PHOTONIC LINKS USING DOUBLE SIDEBAND SUPPRESSED CARRIER MODULATION AND BALANCED COHERENT HETERODYNE DETECTION

Charles Middleton and Richard DeSalvo, *Senior Member, IEEE*
Harris Corporation
Melbourne, FL

ABSTRACT

Optical transmission of microwave signals offers many advantages such as increased bandwidth; immunity to electromagnetic interference; reduction of size, weight and power consumption; and low, frequency-independent loss over long distances. But microwave photonic links often lack the performance required to replace traditional microwave links. We present a microwave photonic link architecture that enables high gain and dynamic range, low noise figure, and multi-octave bandwidth operation. Our method uses double sideband suppressed carrier modulation together with a balanced coherent heterodyne detection scheme. The modulation method increases link linearity by producing amplitude modulation based on the optical field rather than intensity. The combination of carrier suppression, optical amplification, phase-locked local oscillator insertion, and balanced detection provide high signal-efficient gain, reduced intermodulation distortion, wide-band operation, and low link noise. The resulting link places this microwave photonic approach in the same performance realm as state-of-the-art microwave links.

INTRODUCTION

Analog photonic links with ultra-high linearity, sensitivity and dynamic range over large bandwidths are required for challenging, signal-rich military environments. Conventional intensity-modulated direct detection (IM/DD) methods are limited in performance by the linearity of the modulator. We present an analog photonic link using coherent heterodyne detection and advanced noise and intermodulation suppression techniques to significantly increase linearity and dynamic range over the current state of the art. Our approach is based on a novel double sideband-suppressed carrier (DSB-SC) modulation technique and a heterodyne balanced receiver [1].

Many works have been developed around the use of carrier subtraction techniques to improve the dynamic range of RF photonic links. The techniques range from low-biasing modulators, filtering the DC optical carrier using narrow-bandwidth FBGs, or a combination of both [5-8] to the use of coherent carrier suppression techniques [9]. 10 dB improvements in link efficiency and moderate increases in the SFDR (117 dB-Hz$^{2/3}$) are reported, but unless a method is employed to reduce the second-harmonic component that arises from these suppression methods, the links are relegated to sub-octave applications. Moreover, if high RF powers are required, the carrier suppression leads to low RF conversions. Coherent carrier reinsertion through the use of a local oscillator has demonstrated improved RF performance along with high dynamic ranges (121 dB-Hz$^{2/3}$) [2, 3]. Ryu and Horiuchi show that in a pre-amplifier application a low noise optical amplifier is effective for improving the performance of a receiver which operates in a thermal-noise dominant condition [10].

We have chosen DSB-SC modulation for the translation to lightwave frequencies over that of conventional IM/DD since it provides the means of delivering high optical powers with larger RF signal content, as well as the benefits of coherent gain. Carrier suppression significantly reduces the noise contributions due to the DC optical bias when compared to conventional amplitude modulated (AM) coherent links [2]. Finally, the use of balanced detection provides the last step in noise reduction while also providing increased signal gain.

To achieve DSB-SC modulation, we use a balanced bridge Mach-Zehnder modulator (MZM) specially configured for null biasing for suppression of the optical carrier. In such a configuration, only linear signal-carrying sidebands and odd-order electric-field components exit the “dark” sideband port of the balanced bridge MZM. This provides high inherent link SNR by reducing noise contributors associated with the DC optical carrier component: signal shot noise and beat noise between the signal and amplified spontaneous emission (ASE) from an optical amplifier.

This also provides signal-efficient amplification for the sideband optical pre-amplifier, since gain is primarily transferred to the signal sidebands rather than saturating on the DC optical carrier, reducing overall DC power consumption.

Coherent heterodyne balanced detection provides additional advantages to link performance. Link gain and dynamic range are fully optimized using a low-noise, phase-locked local oscillator laser. This phase locked source can be tuned in frequency to provide RF to IF frequency translation for wide bandwidth performance with a common platform. Balanced detection also provides reduction of even-order inter-modulation distortion (IMD) terms and common-mode noise terms: relative intensity noise (RIN) from both laser sources, as well as signal-ASE and ASE-ASE beat noise. A block diagram of the coherent heterodyne balanced detection link is shown in Figure 1.

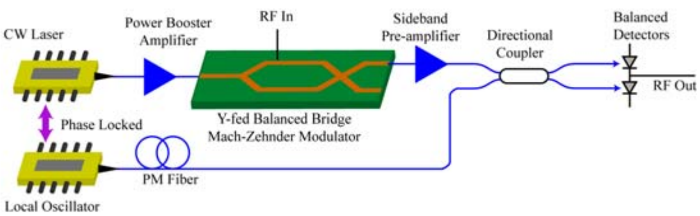

Figure 1 Block diagram of DSB-SC coherent heterodyne microwave photonic link.

In this work we provide theoretical analysis of this link architecture and discuss the required conditions for optimal link performance (SFDR greater than 127 dB $Hz^{2/3}$, positive link gain, noise figure below 6 dB, and OIP2 greater than 70 dB). Since the phase-locked optical source needed for total link characterization is currently being developed, we present experimental results demonstrating many aspects of predicted link performance: suppression of the optical carrier, rejection of the 2^{nd} harmonic, and operation of the heterodyne balanced detector.

THEORY

Suppressed carrier modulation is achieved by biasing a Mach-Zehnder modulator (MZM) such that the carrier components cancel at the output coupler of the modulator, as shown in Figure 2. When we DC bias the modulator at $V_b = V_\pi$, the electric field strength is linearly related to the input voltage. The carrier component exits the dark output port, and the sidebands of the modulated signal exit the signal output port. Thus the output from the signal port is DSB-SC modulation.

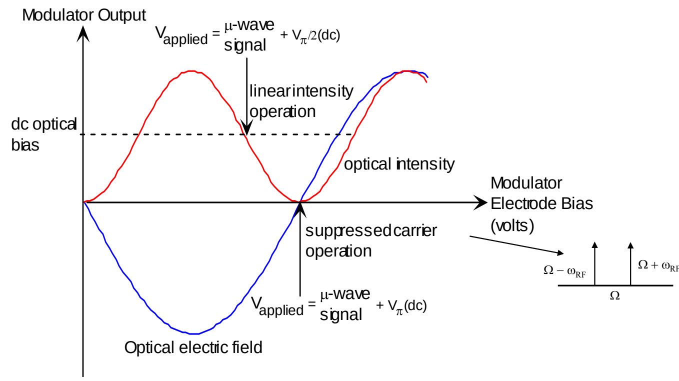

Figure 2: DC bias for DSB-SC modulation

The resultant carrier suppression provides a higher signal-to-noise ratio (SNR) to further reduce the noise contributors associated with the DC optical carrier component, i.e. shot noise and signal-ASE beat noise. Carrier suppression also provides signal-efficient optical amplification primarily on the dominant signal side-bands: the optical amplifier will not be saturated by the DC optical carrier, so the DC power consumption of the amplifier is reduced. Therefore, almost all of the optical power available to the high power-handling photodetectors contributes to signal power with high SNR. This results in an overall gain, noise figure and dynamic range improvement in the DSB-SC link as compared to a similar IM/DD link configuration.

We employ a heterodyne detection method to translate the frequency band of interest in the DSB-SC optical spectrum down to a convenient Intermediate Frequency (IF) by injecting a phase locked local oscillator (LO) laser and mixing with the signal sidebands through an optical directional coupler (see Figure 3). The LO laser is detuned from the carrier to move a particular 4 GHz wide lower sideband channel into the IF bandwidth centered at 2 GHz. This greatly simplifies the receiver design in that fixing the IF at 2 GHz allows the use of a single RF output circuit from the detector, as opposed to a different design for each high frequency channel as would be required for direct-detection links. The upper sidebands are filtered outside the IF filter's 4 GHz bandwidth. Moreover, any residual second-harmonic component of the high-band signal receives additional suppression through the finite bandwidth of the IF filter, further increasing OIP2.

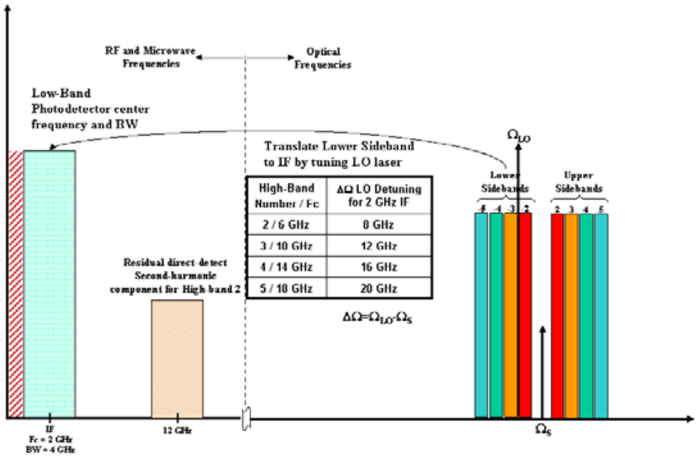

Figure 3: Heterodyne detection approach

The RF conversion gain for a coherent DSB-SC link is proportional to the product of the CW source laser optical power and the local oscillator laser optical power as shown in Figure 4 and Equation 1 below.

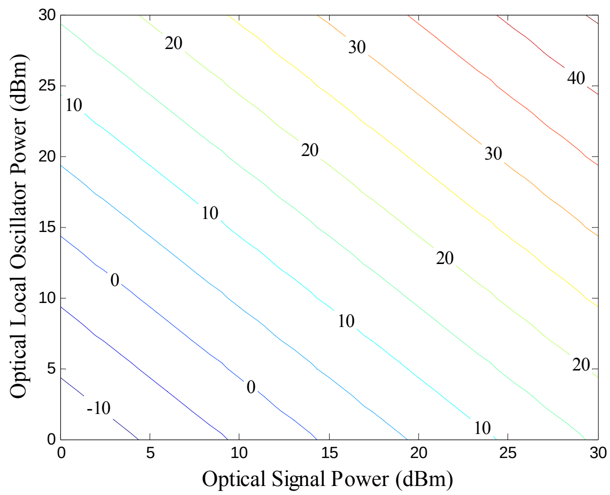

Figure 4: RF conversion gain (dB) as a function of optical signal power and optical local oscillator power.

$$G_{RF} = \Re^2 \frac{P_0 P_{LO}}{2} \left(\frac{\pi}{V_\pi} \right)^2 R_{PD} R_{MZM} \quad (1)$$

High signal power leads to higher conversion gain, and its contribution to the total noise through the DC carrier component is greatly reduced from the carrier suppression. To achieve high source powers, one can employ an Erbium-doped fiber amplifier (EDFA) power booster between the source laser and the modulator. Residual amplified spontaneous emission (ASE) from the booster is reduced through the null-bias, reducing the source laser ASE contributions to the link noise and leading to an overall lower noise figure. Carrier suppression also benefits from sideband pre-amplification immediately after the modulator where the SNR is still at a maximum. In this configuration, we can realize signal efficient amplification of the sidebands since the sideband pre-amplifier does not saturate on the CW optical carrier. This contributes to improvements in the overall link RF performance and improves the DC power consumption through more efficient use of optical gain.

With proper link design, the link noise figure is dominated by the noise terms associated with the local oscillator and by input thermal noise due to positive RF conversion gain. Other noise sources from signal sideband generation are minimized through carrier suppression. Table 1 summarizes the conventional coherent RF photonic link noise terms. Link noise is dominated by input thermal noise and local oscillator shot noise in non-optically amplified configurations, and LO-ASE beat noise when sideband pre-amplifiers are used.

Table 1 Link noise terms arising from the CW source laser and local oscillator laser

	Signal	Local Oscillator
Input Thermal Noise	Contributor	N/A
Shot Noise	Suppressed	Contributor
RIN	Suppressed	Suppressed
Sig/LO-ASE Beat	Suppressed	Contributor
ASE-ASE Beat	Suppressed	Suppressed

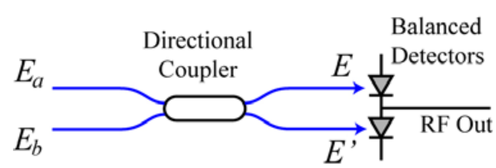

Figure 5: Balanced detection illustration for a coherent link configuration.

Balanced detection provides reduction of common-mode noise terms, i.e. signal-ASE, RIN from CW source laser and LO laser, and ASE-ASE beat noise contributions. Figure 5 illustrates the concept of balanced detection using a directional coupler. The output of the coupler is given by

$$\begin{bmatrix} E \\ E' \end{bmatrix} = \frac{1}{\sqrt{2}} \begin{bmatrix} 1 & i \\ i & 1 \end{bmatrix} \begin{bmatrix} E_a \\ E_b \end{bmatrix} \quad (2)$$

where E_a and E_b are the coupler inputs and E and E' are the coupler outputs. Correlated noise terms and even-ordered intermodulation terms cancel due to balanced detection, and only the uncorrelated noise terms remain. The dominant noise source at E_a is the ASE from the sideband pre-amplifier, n_{ASE}. At E_b, the primary noise contributor is the LO power, which leads to shot noise and LO-ASE beat noise. The output of the coupler is then

$$\begin{bmatrix} E \\ E' \end{bmatrix} = \frac{1}{\sqrt{2}} \begin{bmatrix} 1 & i \\ i & 1 \end{bmatrix} \begin{bmatrix} n_{ASE} \\ E_{LO} \end{bmatrix}. \quad (3)$$

Therefore, local oscillator-associated noise is the dominant contributor to link noise in a suppressed carrier architecture.

Improvements in the link SFDR are realized through the combined improvement in OIP3 and link noise reduction. The OIP3 for a coherent link is proportional to the product of the CW source laser optical power and the LO laser optical power just as described earlier for the RF conversion gain. A judicious balance of LO power and CW source power is used to obtain the required link performance specified for certain applications. Table 2 shows a comparison calculation between a balanced IM/DD link and a balanced DSB-SC. Here it was assumed a modulator half-wave voltage of $V_\pi = 5$ V, laser RIN of -160 dB/Hz, detector responsivity of 0.8 A/W, a common-mode rejection ratio of 20 dB, and a maximum of 10 mA photo-generated current from each balanced detector. LO shot noise was the dominant contributor to the balanced DSB-SC noise figure while signal shot noise was the dominant contributor in the balanced IM/DD link.

Table 2: Calculated performance comparison of a balanced IM/DD link and a balanced DSB-SC link.

	Balanced IM/DD (P_0 = 50 mW)	Balanced DSB-SC (P_0 = 250 mW, P_{LO} = 12 mW)
Gain	-4 dB	+7 dB
NF	19 dB	18 dB
OIP3	19 dBm	33 dBm
SFDR	116 dB $Hz^{2/3}$	121 dB $Hz^{2/3}$

The OIP2 performance of the link is driven by the second-harmonic component that is generated with the MZM is biased at the null to generate suppressed carrier. The suppression of the second-order nonlinearity is governed by the beam-to-beam amplitude and phase accuracy between our balanced detectors and requires <1% to achieve OIP2 > 75.6 dBm. The balance accuracy is also required to achieve additional noise contributor suppression for the source RIN and LO RIN and common path signal-ASE beat noise.

SFDR performance is driven by the OIP3 and the noise floor of the link, where both are optimized through the judicious choice of sideband optical power and LO optical power. Moderately high RF conversion gain drives the link to beat noise limited operation, while the higher conversion gain would force the link to be input thermal noise limited. Carrier suppression is critical not only to reduce the signal-dependent noise, but to provide signal-efficient optical amplification to reduce DC power consumption. Suppressed carrier biasing also helps to attenuate the ASE noise from the source booster EDFA and minimizes the LO-ASE beat noise for overall low-noise receive performance.

Figure 6 shows the SFDR and noise figure as a function of local oscillator power. To achieve SFDR of 127.3 dB $Hz^{2/3}$, implementation of carrier suppression requires the use of a modulator bias controller to compensate for bias drift and provide less than 0.1% bias error. Power booster amplification of 13 dB and sideband pre-amplification of 12 dB are used to provide sufficient signal gain. Contour plots of noise figure (Figure 7) and SFDR (Figure 8) as a function of both optical signal power and optical local oscillator power also show that within a certain range of local oscillator power, increased optical signal power has a more direct impact on link performance than local oscillator power because it increases link gain without increasing link noise, due to carrier suppression and balanced detection. As the local oscillator power increases, input thermal noise and LO-ASE beat noise dominate the link and performance degrades.

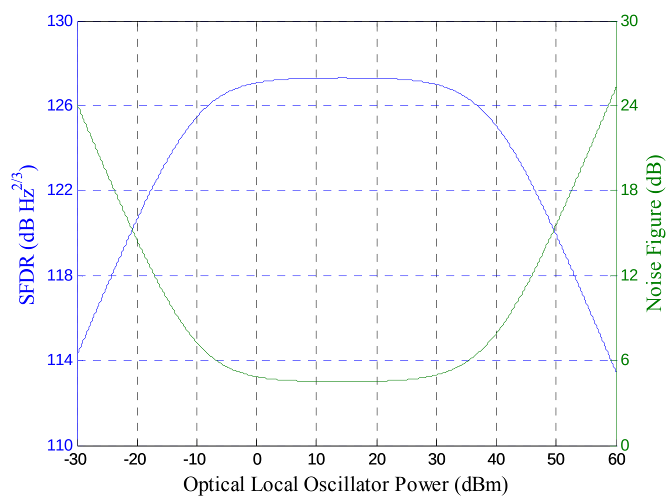

Figure 6: SFDR and noise figure.

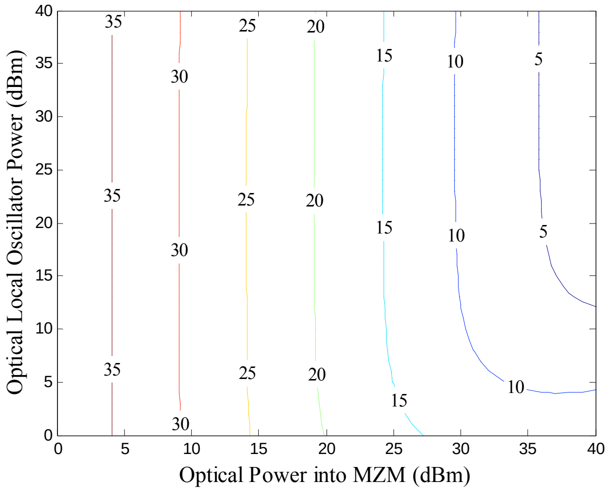

Figure 7: Link noise figure (dB) as a function of optical signal power and optical local oscillator power.

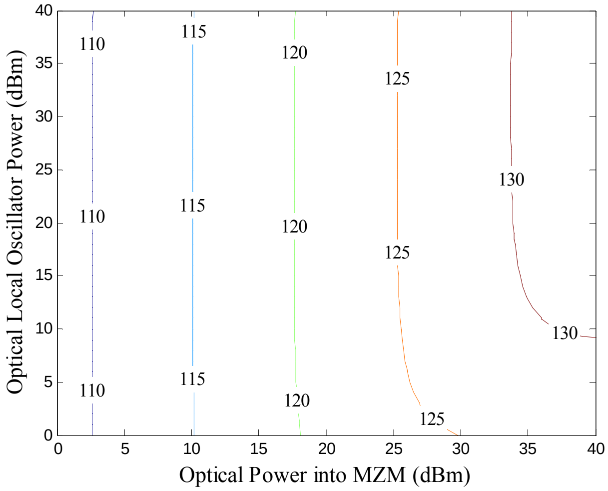

Figure 8: Spur-free dynamic range (in dB $Hz^{2/3}$) as a function of optical signal power and optical local oscillator power.

EXPERIMENTAL RESULTS

As we are currently working to complete the development of the phase-locked laser sources required for this experiment, we have verified several important aspects of this approach. To observe the suppression of the optical carrier with null-biasing of the MZM, we used an optical spectrum analyzer to measure the carrier and sideband powers, as shown in Figure 9. Control of the polarization state of the laser signal entering the MZM is essential in order to achieve a large amount of optical carrier suppression.

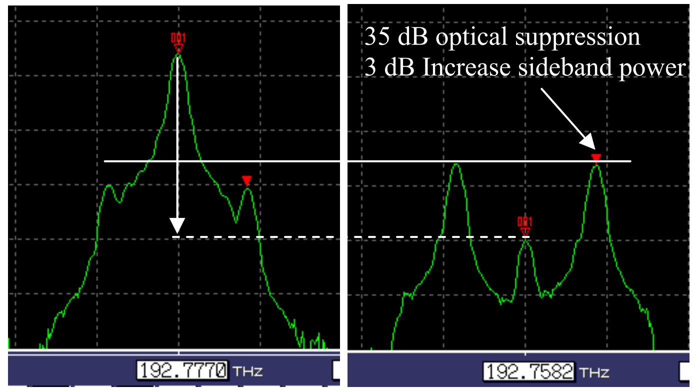

Figure 9: Carrier suppression observed on optical spectrum analyzer

The use of balanced detection provides suppression of common-mode noise terms as well as even-order nonlinearities. To observe the degree of suppression, we measured the second harmonic of a 10 GHz input signal using a single detector and a balanced detector. As shown in Figure 9, careful balancing of the amplitude and phase of the output of the two coupler arms resulted in over 50 dB of suppression.

The introduction of a local oscillator (albeit without phase locking) demonstrates the heterodyne detection principle. Figure 11 shows the suppressed-carrier signal and local oscillator as measured by an optical spectrum analyzer. By temperature-tuning the local oscillator wavelength relative to the optical carrier wavelength, we can produce a down-converted signal at a chosen IF frequency, as shown in Figure 12.

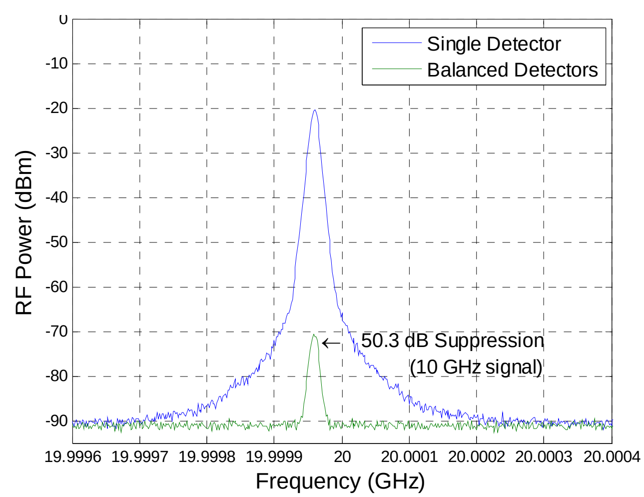

Figure 10: Suppression of 2nd harmonic through balanced detection

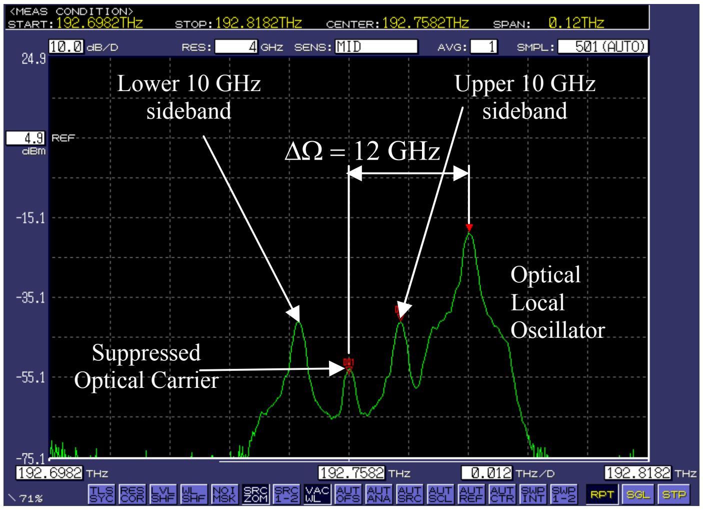

Figure 11: Optical spectrum of carrier-suppressed signal and local oscillator

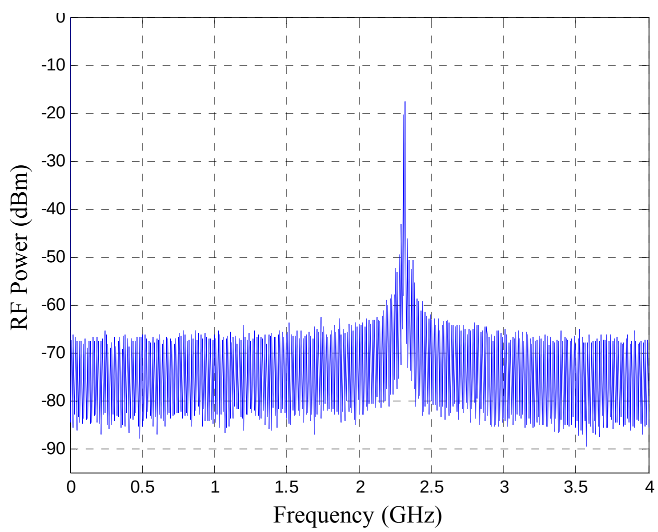

Figure 12: Downconverted X-band signal at IF frequency

CONCLUSION

The use of DSB-SC modulation with coherent heterodyne balanced detection provides low noise, high gain, and high dynamic range link performance. Carrier suppression improves the linearity of the link by operating on the electric field rather than the intensity of the signal, reducing the noise terms associated with the DC optical carrier and providing signal-efficient gain from optical amplification. Coherent heterodyne detection allows the use of a common detector platform to address a wide range of RF frequencies, and provides the phase reference for the sidebands of the carrier-suppressed signal. Balanced detection reduces common-mode noise terms and even-order nonlinearities. This requires the use of two phase-locked laser sources, a balanced bridge MZM, polarization-maintaining optical amplifiers, an optical coupler, and balanced detectors. The optimization of the performance of these components relies on accurate control of polarization states, modulator biasing, and amplitude and phase difference between the balanced detectors. An integrated device could include electronic control of these parameters and meet the demanding requirements of microwave links while reducing size, weight and power consumption.

REFERENCES

[1] Montgomery, R. and R. DeSalvo, "A novel technique for double sideband suppressed carrier modulation of optical fields," IEEE Photonics Technology Letters, 7(4), 434-436 (1995).
[2] Farwell, M., Chang, W., and Huber, D., "Increased linear dynamic range by low biasing the Mach-Zehnder modulator," IEEE Photonics Technology Letters, 5(7), 779-782 (1993).
[3] Esman, R. and Williams, K., "Wideband efficiency improvement of fiber optic systems by carrier subtraction," IEEE Photonics Technology Letters, 7(2), 218-220 (1995).
[4] LaGasse, M., Charczenko, W., Hamilton, M.C., and Thaniyavarn, S., "Optical carrier filtering for high dynamic range fibre optic links," Electronics Letters, 30(25), 2157-2158 (1994).
[5] Meng, X. and Karim, A., "Microwave Photonic Link with Carrier Suppression for Increased Dynamic Range," Fiber and Integrated Optics, 25, 161-174 (2006).
[6] Lindsay, A., "An analysis of coherent carrier suppression techniques for photonic microwave links," IEEE Transactions on Microwave Theory and Techniques, 47(7), 1194-1200 (1999).
[7] Funk, E., Urick, V., and Bucholtz, F., eds, "High dynamic range, long haul (> 100 km) radio over fiber," [Microwave Photonics, ed. C.H. Lee], CRC Press, Boca Raton, 185-212 (2007).
[8] Kalman, R.F., Fan, J.C., and Kazovsky, L.G., "Dynamic range of coherent analog fiber-optic links," IEEE Journal of Lightwave Technology, 12(7), 1263-1277 (1994).
[9] Ryu, S. and Horiuchi, Y., "Use of an optical amplifier in a coherent receiver," IEEE Photonics Technology Letters, 3(7), 663-665 (1991).
[10] Wu, Y., B. Xie, J. H. Hodiak, S. M. Lord, and P. K. L. Yu, "Multioctave High Dynamic Range Up-Conversion Optical-Heterodyned Microwave Photonic Link," IEEE Photonics Technology Letters, 16(10), 2332-2334 (2004).